Inverse Problems in Engineering : Theory and Practice
3rd Int. Conference on Inverse Problems in Engineering
June 13-18, 1999, Port Ludlow, WA, USA

HT05

HEAT FLUX ESTIMATION IN THIN-LAYER DRYING

Olivier Fudym **Christine Carrère-Gée** **Didier Lecomte** **Bruno Ladevie**

Ecole des Mines d'Albi, Centre Energétique –Environnement
Route de Teillet, 81013 Albi, France,
33 (0) 5 63 49 30 24 – fudym@enstimac.fr

ABSTRACT

A method is developed in order to determine the drying curves for sludge thin-layer drying. Since mass balance is very difficult to measure for thin-layer drying, these curves are obtained through energy balance. An experimental device is built up, in order both to provide and to estimate the heat flux density at the interface between a hot metallic plate and the drying sample. An analytical direct model is made using the quadripole formalism, and the system transfer function is calculated. The inverse problem is solved using the beck's sequential function specification method, and the corresponding drying curve is deduced by a simple energy balance. Real experiment results are presented.

INTRODUCTION

Among contact drying technologies, drum drying is widely used in the food industry, to treat heat-sensitive products. It also presents a great interest for sludge drying. The product is sprinkled or coated on a hot rotating cylinder. The wall temperature is above boiling temperature. Absence of mixture and agitation constitutes an advantage for viscous products like sludge, enabling a good control of residence time, averaged water content and thermal efficiency. For contact dryer's design, it is important to predict drying rates, but this rate is limited by internal conductive transfers. It is then necessary to find a maximum ideal reference, not driven by internal transfers, but by the intrinsic product's thin film boiling rate : this is the main scope of this paper. The present study's application is for sludge drying.

In a previous work, it was shown by Vasseur (1983) that very high heat flux are exchanged during the first instants for viscous foodstuff thin film drying, due to the low product's thickness.

NOMENCLATURE

A, B, C, D	Quadripole elements
F(s)	Transfer Function
X	Moisture content
Y	Measured temperature
M	Dry matter load
f(t)	Inverse transfer function
dt	Time step
q	Interface heat flux density
T	Computed Temperature
a	Thermal diffusivity
l_v	water latent heat
r	Future time steps number
s	Laplace variable
t	Time
b	Thermal effusivity
e_1	Sensor location
e	Plate thickness
ε_2	$e - e_1$
λ	Thermal conductivity
φ	Heat flux density
ϕ	Laplace Tr. heat flux
θ	Laplace Tr. temperature
ρc_p	Volumetric thermal capacity

Mass rate drying, when involved in a vaporization thin film process, is very difficult to measure :

- Boiling transfer is a rather stochastic and violent phenomena, and highly fast for thin film boiling
- Mass losses are difficult to measure, because very little material is coated on the wall

- Product's sampling is made impossible, because drying rate is too high.

Since mass balance can't be directly known, a way to estimate the drying rate is doing an energy balance, assuming that the amount of energy involved in vaporization drying is known. It is thus necessary to obtain reliable values of the interface heat flux between the drying product and the heated surface.

The experimental device, developed for this study, is presented in next section.

1. Experimental device

The first objective of this experimental device is to produce thermal conditions for thin film vaporization contact drying. The product's thin-layer (about 0.7 mm thickness) is coated on a hot metallic plate. The plate must be thick enough in order to store the energy amount necessary for complete drying (58 mm thickness). It must be highly diffusive in order to ensure high heat flux densities at the interface. The heat is stored at a temperature above boiling temperature and suddenly discharged when the product is coated. Initial temperature is provided by placing the plate in a drying loop.

The second main goal is to estimate the interface heat flux between the drying product and the heated surface. It must be emphasized that no direct surface temperature can be made : a sensor located on the front side would perturb the material coating, as well as heat transfer…Thus wall temperature and flux must be estimated using interior location temperature and an inverse heat conduction method.

A thin thermocouple with separated contacts is dulled inside the plate, near the surface, laid in a direction parallel to isothermal curves. With this particular method, the sensor location is precisely known (fig. 1). Another sensor is laid out on the plate's bottom side (T_2 on fig. 2).

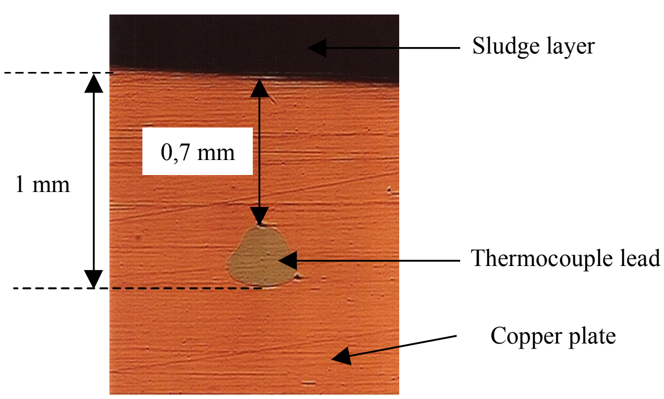

Figure 1 - Sensor dulled inside the plate

2. Direct model

A direct model is built in order to calculate the sensor temperature evolution, when a given heat flux is applied to the plate's surface. The system is shown on fig.2. An analytical one dimensional conductive model is built, assuming that the plate's bottom is insulated. The quadripole formalism (Degiovanni, 1988) is used, and the transfer function $F_1(s)$ between the interface heat flux ϕ and temperature T_1 is calculated.

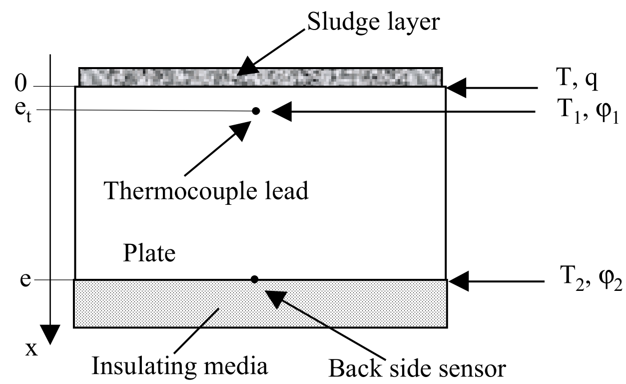

Figure 2 - Schematic Experiment

Heat transfer is here assumed to be purely conductive and the sample homogeneous :

$$\frac{\partial^2 T^*}{\partial x^2} = \frac{1}{a}\frac{\partial T^*}{\partial t} \qquad (1)$$

with a known heat flux density at the plate surface x=0 and insulated bottom at x=e.

Initially, the whole system is assumed to be at uniform temperature T_0. A new variable is then considered such as $T=T^* - T_0$.

To write the previous system in a quadripole form, Laplace transform is applied. Equation (1) becomes an ordinary differential equation :

$$\frac{d^2\theta}{dx^2} = \frac{s}{a}\theta \qquad (2)$$

with heat flux definition such as

$$\phi(x,s) = -\lambda \frac{d\theta(x,s)}{dx} \qquad (3)$$

Expressions (2) and (3) are then equivalent to a quadripole presentation (Batsale, 1994) such as

$$\begin{bmatrix}\theta \\ \phi\end{bmatrix} = \begin{bmatrix}A_1 & B_1 \\ C_1 & D_1\end{bmatrix}\begin{bmatrix}\theta_1 \\ \phi_1\end{bmatrix} \qquad (4)$$

$$\begin{bmatrix}\theta_1 \\ \phi_1\end{bmatrix} = \begin{bmatrix}A_2 & B_2 \\ C_2 & D_2\end{bmatrix}\begin{bmatrix}\theta_2 \\ 0\end{bmatrix} \qquad (5)$$

where (i=1,2) :

$$A_i = D_i = ch(k.e_i) \quad (6)$$

$$B_i = \frac{sh(k.e_i)}{k\lambda} \quad (7)$$

$$C_i = k\lambda sh(k.e_i) \quad (8)$$

and $$k = \sqrt{\frac{s}{a}} \quad (9)$$

It is then easy to determine the transfer functions $F_i(s)$ between the Laplace transformed superficial heat flux ϕ, and the temperatures θ_i to be calculated by

$$\theta_i = F_i(s).\phi \quad (10)$$

Inverse method allows to calculate the superficial heat flux density q(t) from the measured temperatures Y_1 (t) at sensor location, and corresponding temperature T_1 (t) from the direct model. Inverse transfer function $f_i(t)$ are obtained from F_i (s) through a numerical Laplace inversion (Stehfest, 1970).

The temperature $T_i(t)$ is then calculated by a convolution product :

$$T_i(t) = \int_0^t q(t-\tau).f_i(\tau)d\tau \quad (11)$$

Of particular interest is the transfer function between q(t) and the computed temperature $T_1(t)$ at sensor location :

$$F_1(s) = \frac{A_2}{C_1 A_2 + D_1 C_2} \quad (12)$$

The insulated boundary condition will be validated from back side measurements Y_2 (T_2 location). Nevertheless, it would be possible to integrate these values in the boundary condition's knowledge.

3. Inverse method

In the case of one dimensional problem with fast and high heat flux changes, a sequential method is adapted. The function specification method, with a sequential constant heat flux functional form is used (Beck, 1970).

For that method (Beck, 1985) , q(t) is approximated in a discrete form :

$$q = [q_1 \quad q_2 \quad .... \quad q_i \quad q_{i+1} \quad .... \quad q_n] \quad (13)$$

where $q_i = q(t_i) = q(i.dt)$. Equation (11) can be expressed in a discrete form :

$$T_i = T(t_i) = \sum_{j=1}^{i} f_1(t_i - t_j).q_j.dt$$
$$= dt.[q_1 f_i + q_2 f_{i-1} + ... + q_{i-1} f_2 + q_i f_1] \quad (14)$$

with $f_j = f_1(t_j)$.

Assuming that q_1--------q_i and T_1-------T_i are known, q_{i+1} is searched by an ordinary least square procedure using the next Y_{i+1} -------Y_{i+r} measurements, assuming a constant heat flux q_{i+1} during the r future time steps (Fig.3) :

$$q_i = q_{i+1} = q_{i+2} = ... = q_{r-1} = q_r \quad (15)$$

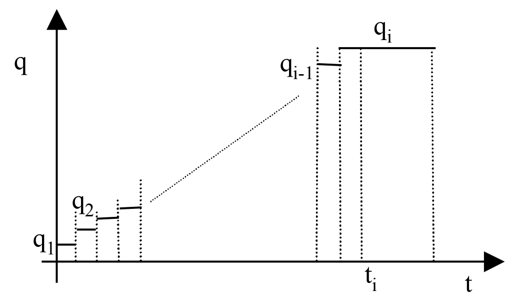

Figure 3 - Time discretization at time step ti

The least squares procedure minimizes the functional form J with respect to q_{i+1} :

$$J(q_{i+1}) = \sum_{j=1}^{r} \left(Y_{i+j} - T_{i+j}(q_{i+1})\right)^2 \quad (16)$$

Equation (16) is differentiated with respect to q_{i+1} and set equal to zero :

$$\frac{\partial J(q_{i+1})}{\partial q_{i+1}} = -2 \sum_{j=1}^{r} \left(Y_{i+j} - T_{i+j}(q_{i+1})\right) \frac{\partial T_{i+j}}{\partial q_{i+1}} = 0 \quad (17)$$

The heat flux increment during the time step is searched :

$$q_{i+1} = q_i + \delta q \quad (18)$$

Thanks to Eq. (15), the r future computed temperatures T_{i+j} (q_{i+1}) can be written as :

$$T_{i+j}(q_{i+1}) = T_{i+j}(q_i) + \frac{\partial T_{i+j}}{\partial q_i}\delta q \quad (19)$$

and for the same reason ($q_i = q_{i+1}$), the sensitivity coefficients in Eq. (17) and Eq. (19) are equal :

$$S_{i+j} = \frac{\partial T_{i+j}}{\partial q_{i+1}} = \frac{\partial T_{i+j}}{\partial q_i} \quad (20)$$

Equations (17 – 20) yield to the heat flux increment δq for q temporarily assumed constant (Eq. 21). This equation is used in a sequential manner by increasing i by one each time step.

$$\delta q = \frac{\sum_{j=1}^{r} \left(Y_{i+j} - T_{i+j}(q_i)\right) S_{i+j}}{\sum_{j=1}^{r} S_{i+j}^2} \qquad (21)$$

The sensitivity coefficients defined in Eq. (21) are known from Eq. (14) with i replaced by i+1 to i+r. For example, the temperature T_{i+j} at time t_{i+j}, with assumption of constant heat flux after time t_i, can be expressed as :

$$T_{i+j} = dt.\left[q_1 f_{i+j} + q_2 f_{i+j-1} + \ldots + q_{i+j-1} f_2 + q_{i+j} f_1\right] \quad (22)$$

Assuming Eq. (15) yields to the sensitivity coefficients, with j = 1 to r :

$$S_{i+j} = dt.\left[f_1 + f_2 + \ldots\ldots\ldots\ldots\ldots\ldots + f_{i+j-1} + f_{j+1}\right] \qquad (23)$$

It is shown the great interest that have a direct model with a convolution such as Eq. (11) coupled with the specification function method : the sensitivity coefficients are constant with time step, and only the first r+1 values of the inverse transfer function are to be calculated. The sum of inverse transfer function values in Eq. (23) also imply a growing behavior for these sensitivity coefficients. This fact improves the future time steps stabilization effect in Eq. (21), because each future time step number increment will contribute with a sensitivity coefficient growth. Sensitivity analysis is to be detailed in next section.

4. Sensitivity analysis

The direct model, described in section 2, is used with a heat flux functional form similar to experimental results. Reduced sensitivity coefficients to the main parameters are plotted on fig. (4). It is shown that sensitivity of T_1 to e_1 is very low. This is due to the sensor location, near to the surface.

Sensitivity coefficients to thermal conductivity and thermal diffusivity are the same order than sensitivity to mean heat flux gain ϕ_0. It is then important to get good knowledge of the plate's thermal properties.

Equation (14) can be written in a matrix form, in order to express the sensitivity matrix **X** to the unknown heat flux components :

$$\mathbf{T} = \mathbf{X}\mathbf{q} \qquad (24)$$

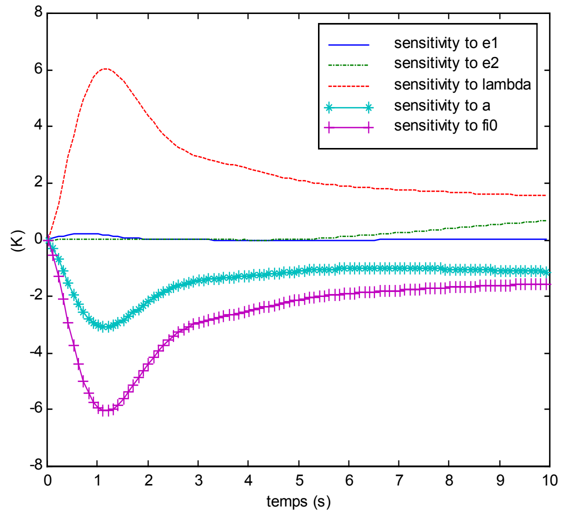

Figure 4 – Reduced sensitivity coefficients

A whole time domain estimation procedure would be difficult to regularize : The q_i component at time t_i can be estimated only very close to time t_i.

$$\mathbf{X} = dt.\begin{bmatrix} f_1 & 0 & 0 & \ldots & \ldots & \ldots & 0 \\ f_2 & f_1 & 0 & \ldots & \ldots & \ldots & 0 \\ f_3 & f_2 & f_1 & 0 & \ldots & \ldots & 0 \\ . & f_3 & f_2 & f_1 & \ldots & \ldots & . \\ . & \ldots & \ldots & \ldots & .. & \ldots & . \\ . & & & . & . & f_1 & 0 \\ f_n & \ldots & \ldots & \ldots & f_3 & f_2 & f_1 \end{bmatrix} \qquad (25)$$

The dirac form of sensitivity coefficients to q can be understood with Eq. (25), and is due to the deep exponential decrease of the transfer function f(t).

Sensitivity coefficients, obtained from Eq. (24 - 25) are presented on a map by fig. (5). It is shown that the sensitivity coefficient is non zero only for a very few points very close to each heat flux component q_i at time t_i.

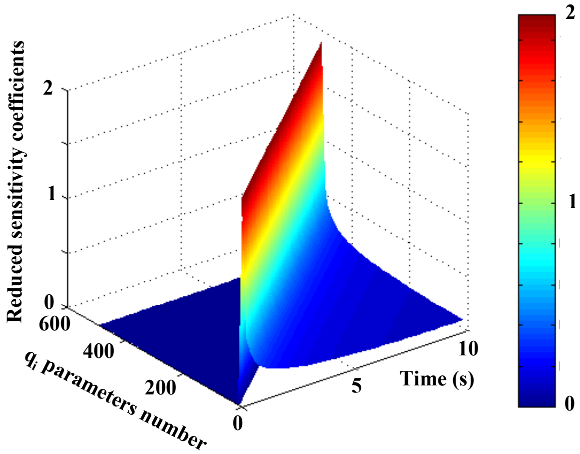

Figure 5 – Sensitivity coefficients map

The comparison between fig. (5) and fig. (6) makes clear the present algorithm interest, and the future time steps stabilization effect, since the sensitivity coefficients curve shown by fig. (6) is a growing function with the future time steps number.

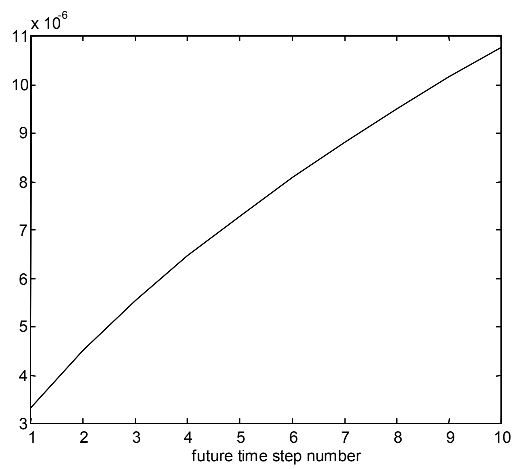

Figure 6 – Future time step sensitivity coefficients for the sequential method : S_{i+j}, j = 1 to r (Eq. 23)

5. Heat flux estimation results

Some method's validation tests have been implemented with "numerical experiments", and have proved its efficiency, but the corresponding results are not presented herein. In this section, only real experiment results are shown.

The plate is placed inside a drying loop, and a stable initial temperature above the product's boiling temperature is reached before the experiment is started. At time 0, the product is quickly coated on the plate, while Y_1 and Y_2 acquisition goes on.

Although a lot of experiments have been made, the goal of the present paper is only to present the general work and method, and the results are exhibited only for one case, with initial temperature T_0 equal to 138 °C.

Time step is dt = 0.01 s., the estimated parameters number is 2518, and the future time steps number r is 5.

Measured and computed temperatures evolution are plotted on fig. (7). The measured sensor temperature Y_1 is perfectly fitted with T_1 , but this is directly due to the inverse method, very close to an exact matching algorithm. More important is the perfect fit between back side measurement Y_2 and computed temperature T_2, because this means a good concordance between the experiment and the model, and proves the validity of back side insulated boundary condition assumption. Wall temperature T and T_1 are almost identical, due to the low distance e_1 and the copper's high thermal conductivity.

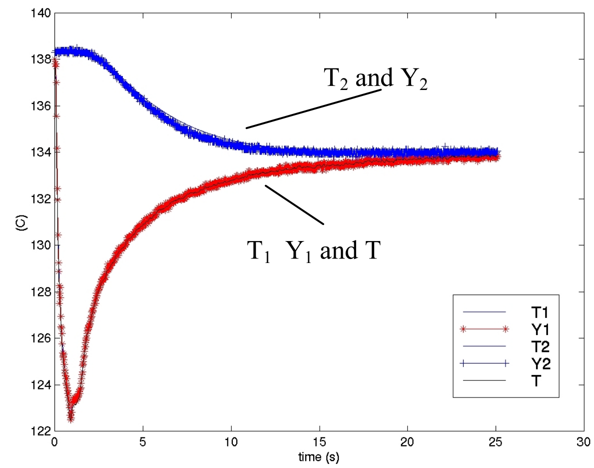

Figure 7 – Computed and measured temperatures

Y_1 is submitted to a straight diminution due to sudden boiling phenomena, and the corresponding superficial high heat flux density. The decrease is stopped when the heat flux intensity falls down while thermal diffusion inside the copper plate tends to its homogenization. When q(t) is near to zero, front side and back side temperatures tend to the same value, corresponding to a quasi-permanent state.

The wall temperature T is always above product's boiling temperature. Boiling transfer stops probably due to the product structure evolution : a high external thermal resistance is found between the dried product and the plate interface.

Figure (8) indicates superficial heat flux density q(t) estimated from Y_1 measurements and inverse procedure. A high value, about 10^6 W.m^{-2} is raised after a very short time smaller than one second, due to boiling phenomena. The flux decrease occurs when boiling drying stops, and is followed by an evaporative drying period, involving smallest heat transfer (about 10^3 W.m^{-2}).

The main objective of thin-layer drying is to dry most of product with boiling drying. The transient period between boiling and evaporation drying is more or less defined. When initial temperature T_0 is near to the product's boiling temperature, this transient period is large.

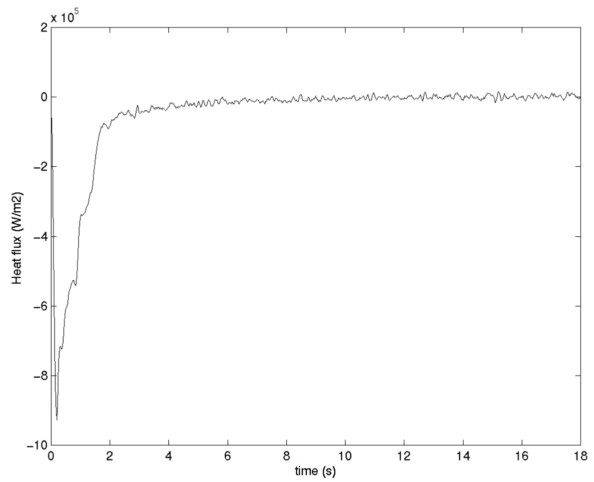

Figure 8 – Estimated superficial heat flux density q(t)

Assuming the classical statistical description of temperature measurement errors (Beck, 1977), it is possible to estimate the corresponding standard deviations. For the present experiments, the standard deviation σ_T for temperature measurements is found to be about 0.07 °C. Estimated heat flux standard deviation σ_q is plotted on fig. (9) as a function of the future time steps number r. The decay is due to the stabilization effect of growing r (see on fig. 6).

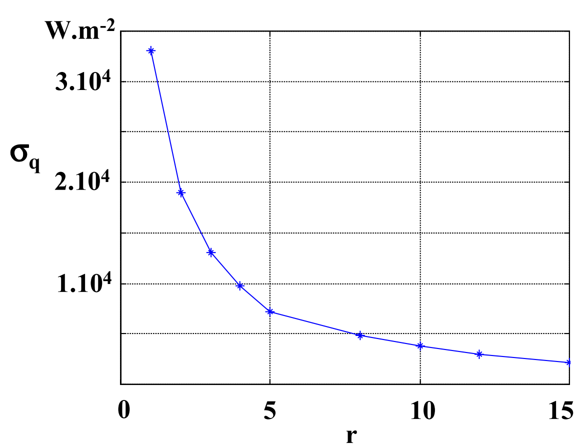

Figure 9 – Estimated heat flux standard deviation σ_q as a function of the future time steps number r.

6. Energy balance and drying curves

Superficial heat flux knowledge can be used to calculate the energy density E lost through the surface :

$$E(t) = \int_0^t q(\tau)d\tau \tag{26}$$

The global energy density lost by the copper plate after a new quasi-permanent state is reached (when front side and back side temperatures are equal to T_f) is :

$$E' = \rho c_p .e.(T_f - T_0) \tag{27}$$

E' is found to be quite close to $E(t_f)$, where t_f is the final time when $T_1=T_2=T_f$. This means that q(t) is the unique flux cruising plate walls. This fact confirm the insulated back side assumption, but also seems to prove there are no lateral losses, hence the one dimensional conductive transfer assumption is valid.

It is now possible to calculate the dry matter load :

$$M = \frac{E'}{(X_0 - X_f)l_v} \tag{28}$$

with X_0 and X_f initial and final moisture content. It is very important to know precisely the dry matter load M, since drying rate is highly dependant on this quantity, and it is not possible to deduce its value with direct experimental measurements.

The moisture content X(t), the drying curves, and finally the drying rate can be deduced from Eq. (26 - 28) :

$$X(t) = X_0 - \frac{E(t)}{M.l_v} \tag{29}$$

$$\frac{dX}{dt} = -\frac{q(t)}{M.l_v} \tag{30}$$

Drying curves are shown by fig. (10). It is noticeable that boiling thin-layer drying, in that particular case, is very fast, thanks to the non internal transfer limitation. The global drying time is increasing with initial temperature.

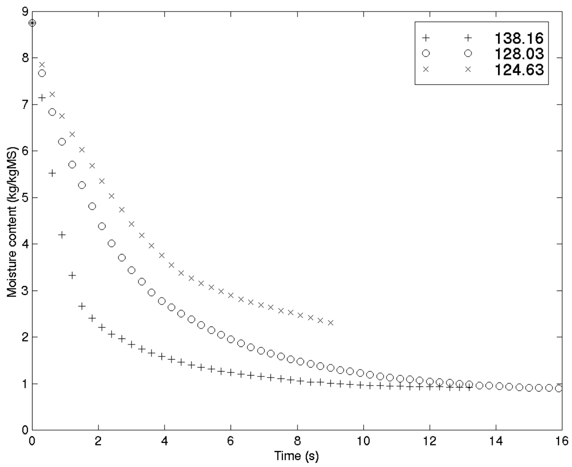

Figure 10 - Drying curves - Initial temperature T_0 effect

CONCLUSION

The present experiment has been developed in order to determine the drying curves for sludge thin-layer drying. Since mass balance is very difficult to measure for thin-layer drying, these curves are obtained through an inverse method used to estimate superficial heat flux density history from internal temperature measurements and energy balance. These curves are used as an ideal reference for drum dryer's design, since industrial dryers always have an internal conductive transfer limitation.

REFERENCES

Vasseur J., Etude du séchage d'un produit visqeux en couche mince sur une paroi chaude, permettant de définir un modèle de séchoir sur cylindre, thèse, 1983.

Degiovanni A., Conduction dans un "mur" multicouche avec sources : extension de la notion de quadripôle, Int. J. Heat Mass Transfer, vol 3, pp 553-557, 1988.

Batsale J.C., D.Maillet, A.Degiovanni, Extension de la méthode des quadripôles thermiques à l'aide de transformations intégrales: calcul de transfert transfert thermique au travers d'un défaut plan bidimensionnel, Int. J. Heat Mass Transfer. Vol 37, pp 111-127, 1994.

Stehfest H., Remarks on algorithm 368. Numerical inversion of Laplace transform, A.C.M, Vol 53, No 10, pp 624, 1970.

Beck J.F., K.J Arnold, Parameters estimation in engineering science, John Wiley & Sons, New York, 1977.

Beck J.F., Nonlinear estimation applied to the nonlinear inverse heat conduction problem, Journal of Heat Mass Transfer, Vol 13, pp 703-716, 1970.

Beck J.F., Blackwell B., St. Clair C., Inverse heat condition, ill-posed problems, Wiley-Interscience, New York, 1985.

Blanc G., Raynaud M., Solution of inverse heat conduction problem from thermal strain measurements, Journal of Heat Transfer, Vol 118, pp 842-849, 1996.